UPCommons

Portal del coneixement obert de la UPC

http://upcommons.upc.edu/e-prints

Aquesta és una còpia de la versió *author's final draft* d'un article publicat a la revista *Journal of the Franklin Institute*.
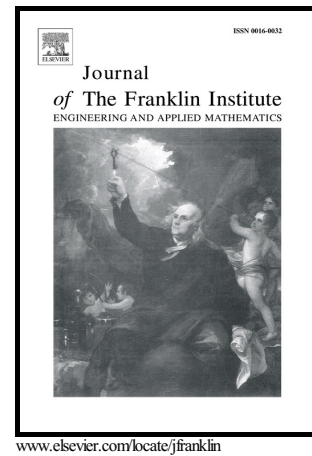
URL d'aquest document a UPCommons E-prints:

http://upcommons.upc.edu/handle/2117/90847

Author's Accepted Manuscript

Stability of Markov jump systems with quadratic terms and its application to RLC circuits

Alessandro N. Vargas, Gisela Pujol, Leonardo Acho

Stability of Markov jump systems with quadratic terms and its application to RLC circuits[☆]

Alessandro N. Vargas[a,1,*], Gisela Pujol[b], Leonardo Acho[b]

[a]*Universidade Tecnológica Federal do Paraná, UTFPR,*
Av. Alberto Carazzai 1640, 86300-000 Cornelio Procópio-PR, Brazil.
[b]*CoDAlab (Control, Dynamics and Applications),*
Departament de Matemàtica Aplicada III, Universitat Politècnica de Catalunya,
Comte d'Urgell, 187, 08036 Barcelona, Spain.

Abstract

The paper presents results for the second moment stability of continuous-time Markov jump systems with quadratic terms, aiming for engineering applications. Quadratic terms stem from physical constraints in applications, as in electronic circuits based on resistor (R), inductor (L), and capacitor (C). In the paper, an RLC circuit supplied a load driven by jumps produced by a Markov chain—the RLC circuit used sensors that measured the quadratic of electrical currents and voltages. Our result was then used to design a stabilizing controller for the RLC circuit with measurements based on that quadratic terms. The experimental data confirm the usefulness of our approach.

Keywords: Stochastic systems; Quadratic systems; Markov jump systems; Stability; Electronic circuits.

1. Introduction

Systems subject to Markovian jumps have received attention in recent years because of their potential for representing processes subject to abrupt variations—see, for instance, some recent applications in economics [6], [16], robotics [21], and direct current (DC) motors [17, 19, 20, 25]. In the linear context, recent contributions for Markov jump systems can be found in the monographs [3, 7] and in the papers [5, 9, 18, 22, 26, 27, 28, 29]; for the nonlinear counterpart, contributions can be found in [14, 23, 24, 32], just to cite a few.

Although characterizing the stability of nonlinear Markov jump systems has been a topic of intensive research [14, 23, 24, 31], little attention has been paid to the stability of quadratic Markov jump systems. In reality, to the best of the authors' knowledge,

[*]Corresponding author
Email address: `avargas@utfpr.edu.br` (Alessandro N. Vargas)

₁₁ this paper is the first to consider quadratic terms for Markov jump systems. Presenting
₁₂ easy-to-check conditions to guarantee the stability of such systems represents the main
₁₃ contribution of this paper.

To clarify our findings, we now formalize the quadratic Markov jump system under
study. Let $(\Omega, \mathcal{F}, \{\mathcal{F}_t\}, P)$ be a fixed, filtered probability space governing the following Itô
stochastic differential equation with Markov jumps:

$$\mathrm{d}x(t) = A_{\theta(t)}x(t)\mathrm{d}t + \begin{bmatrix} x(t)'G_{1,\theta(t)}x(t) \\ \vdots \\ x(t)'G_{n,\theta(t)}x(t) \end{bmatrix} \mathrm{d}t + H_{\theta(t)}\mathrm{d}w(t), \quad \forall t \geq 0, \ x(0) = x_0 \in \mathbb{R}^n, \quad (1)$$

₁₄ where $x(t)$ denotes an n-dimensional system state, $w(t)$ denotes a standard r-dimensional
₁₅ Brownian motion, and $\{\theta(t)\}$ represents an irreducible continuous-time Markov process
₁₆ having $\mathscr{S} = \{1, \ldots, N\}$ as state space. As usual, $x(t)$, $w(t)$, and $\theta(t)$ are mutually indepen-
₁₇ dent random variables at $t \geq 0$. The value of each tuple of matrices $(A_i, H_i, G_{1,i}, \ldots, G_{n,i})$,
₁₈ $i = 1, \ldots, N$, is given.

₁₉ The main contribution of this paper is to present conditions to assure that the quadratic
₂₀ Markov jump system in (1) is second moment stable, as follows.

₂₁ **Definition 1.1.** *([1, Defn. 11.3.1, p. 188]). We say the quadratic Markov jump system*
₂₂ *in (1) is second moment stable if there exists some constant $c = c(x_0)$ such that*

$$\mathrm{E}[\|x(t)\|^2] \leq c, \quad \forall t \geq 0.$$

₂₃ Now, consider the elements of the n-dimensional vector $x(t)$ written explicitly in the
₂₄ form $x(t) \equiv [x_{[1]}(t), \ldots, x_{[n]}(t)]'$.

₂₅ **Assumption 1.1.** *The elements $x_{[\ell]}(t)$, $\ell = 1, \ldots, n$, are uniformly bounded from below*
₂₆ *almost surely. As a result, there exist values $\mu_1, \ldots, \mu_n$ such that*

$$\mu_\ell \leq \liminf_{t \to \infty} x_{[\ell]}(t), \quad \ell = 1, \ldots, n, \quad (2)$$

₂₇ *almost surely.*

₂₈ The condition in Assumption 1.1 is fundamental in our approach. Assumption 1.1
₂₉ states a lower bound for $x_{[\ell]}(t)$, but an upper bound on $x_{[\ell]}(t)$ may not exist, that is, $x_{[\ell]}(t)$
₃₀ could diverge to infinity as t goes to infinity. In order to prevent such divergent behaviour
₃₁ in (1), we present conditions to guarantee the second moment stability, as in Definition
₃₂ 1.1.

₃₃ The assumption that $x_{[\ell]}(t)$ has a lower bound is mild, since there are many applications
₃₄ for which the system states are bounded from below. For instance, in DC motors, both
₃₅ the angular velocity and the electrical current are bounded from below [19, 20].

₃₆ This paper has two contributions. First, the paper shows conditions to assure the sec-
₃₇ ond moment stability of the quadratic system in (1). Second, the paper shows a practical
₃₈ application to an electrical circuit based on resistor (R), inductor (L), and capacitor (C).

39   RLC circuits have the electrical current and the voltage as elements of the system-
40 state—the lower-bounds required by Assumption 1.1 arise from circuits' assemblage, as
41 illustrated in Section 4. Indeed, we used our theoretical result to design a stabilizing
42 Markov jump controller for an RLC circuit in practice. Experiments were carried out, and
43 the corresponding experimental data support our findings.

44   The paper is organized as follows. Section 2 quotes the notation, definitions, and Sec-
45 tion 3 presents the main stability result for the stochastic system (1). Section 4 illustrates
46 our findings through a real-time application for an RLC circuit. Finally, Section 5 presents
47 some concluding remarks.

48 2. Notation and definitions

49   Let us denote the n-dimensional Euclidean space by $\mathbb{R}^n$ and the corresponding Eu-
50 clidean norm by $\| \cdot \|$. The symbol $\text{tr}\{\cdot\}$ denotes the trace operator. The identity matrix
51 on $\mathbb{R}^{n \times n}$ is represented by I_n. The symbol $\mathbb{1}_{\mathcal{C}}$ represents the Dirac measure of $\mathcal{C}$, i.e., $\mathbb{1}_{\mathcal{C}}$
52 equals 1 when the condition $\mathcal{C}$ is true and 0 otherwise. Given two matrices $U \in \mathbb{R}^{n \times n}$
53 and $V \in \mathbb{R}^{m \times m}$, $\text{diag}(V, U)$ represents a square diagonal matrix made up by V and U
54 as entries in its diagonal form. For simplicity, we use the notation $\text{diag}(V_i)_{\{i=1,\ldots,N\}}$ to
55 represent $\text{diag}(V_1, \ldots, V_N)$.

56   Let $\otimes$ be the Kronecker product in such a way that $U \otimes V \in \mathbb{R}^{nm \times nm}$ is the correspond-
57 ing Kronecker matrix [4]. The Kronecker sum is defined as $U \oplus V = U \otimes I_m + I_n \otimes V$. Let
58 $\text{Re}(z)$ denote the real part of the complex number z. Given any matrix $U \in \mathbb{R}^{n \times n}$, $\sigma(U)$
59 represents the spectrum of U; and the largest real part of the eigenvalues of U is referred
60 to as

$$\text{Re}(\lambda_U) := \max\{\text{Re}(\lambda) : \lambda \in \sigma(U)\}.$$

61 When U stands for a set of N matrices, i.e. $U = (U_1, \ldots, U_N)$, we apply the definition

$$\text{Re}(\lambda_U) = \max\{\text{Re}(\lambda_{U_i}), i = 1, \ldots, N\}.$$

62 3. Main result

63   The main result of this paper is presented in the sequence.

64   Let $\Pi = [\pi_{ij}], i, j = 1, \ldots, N$ be the transition rate matrix associated with the Markov
65 process $\{\theta(t)\}$. Accordingly, consider $p_i(t) := P(\theta(t) = i)$, $i = 1, \ldots, N$, $\forall t \geq 0$. Consider
66 the second moment matrix

$$X_i(t) = \text{E}[x(t)x(t)'\mathbb{1}_{\theta(t)=i}], \quad i = 1, \ldots, N, \quad \forall t \geq 0. \tag{3}$$

Consider also the symmetric positive semidefinite matrix $V(t) \in \mathbb{R}^{n \times n}$, solution of the
matrix differential equation

$$\dot{V}_i(t) = V_i(t) \left(A_i + \sum_{\ell=1}^{n} \mu_\ell G_{\ell,i} \right)' + \left(A_i + \sum_{\ell=1}^{n} \mu_\ell G_{\ell,i} \right) V_i(t)$$
$$+ \sum_{j=1}^{N} \pi_{ji} V_j(t) + H_i H_i' p_i(t), \quad i = 1, \ldots, N, \quad \forall t \geq t_0, \tag{4}$$

3

67 with an initial condition $V_i(t_0) \in \mathbb{R}^{n \times n}$, for each $i = 1, \ldots, N$.

68 Now, we are able to present the main result of this paper.

69 **Theorem 3.1.** *Assume that the matrices $G_{1,i}, \ldots, G_{n,i}$, $i = 1, \ldots, N$, are negative semi-*
70 *definite. Then there exists some $t_0 \geq 0$ such that*

$$\mathrm{tr}\{X_i(t)\} \leq \mathrm{tr}\{V_i(t)\}, \quad i = 1, \ldots, N, \quad \forall t \geq t_0, \tag{5}$$

71 *where $V(t)$ satisfies (4) with $V(t_0) = X(t_0)$.*

72 The proof of Theorem 3.1 is available in Appendix.

73 **Remark 3.1.** *Theorem 3.1 assures that $X(t)$ is bounded from above by $V(t)$, for all $t \geq t_0$.*
74 *Due to $\mathrm{E}[\|x(t)\|^2] = \mathrm{tr}\{\mathrm{E}[x(t)x(t)']\} = \sum_{i=1}^{N} \mathrm{tr}\{X_i(t)\}$, we can conclude that the Markov*
75 *jump quadratic system in (1) is second moment stable provided that $V(t)$ is uniformly*
76 *bounded. This conclusion represents the main theoretical novelty of this paper.*

77 The authors of [11, Thm 5.6], [7, Thm. 3.25, p. 52] have introduced a condition that
78 we recall here to check whether $V(t)$ is uniformly bounded. To present such a condition,
79 we define the matrix

$$\mathcal{A} = \Pi' \otimes I_{n^2} + \mathrm{diag}\left(\left(A_i + \sum_{\ell=1}^{n} \mu_\ell G_{\ell,i}\right) \oplus \left(A_i + \sum_{\ell=1}^{n} \mu_\ell G_{\ell,i}\right)\right)_{\{i=1,\ldots,N\}}. \tag{6}$$

80 **Proposition 3.1.** *([11, Thm 5.6], [7, Thm. 3.25, p. 52]). If $\mathrm{Re}(\lambda_\mathcal{A}) < 0$, then the limit*
81 $\lim_{t \to \infty} V(t)$ *in (4) does exist and does not depend on the initial condition $V(t_0) \in \mathbb{R}^{n \times n}$.*

82 The existence of $\lim_{t \to \infty} V(t)$ assures that $V(t)$ is uniformly bounded. This conclusion,
83 together with Theorem 3.1, Remark 3.1, and Proposition 3.1, allows us to present the next
84 result.

85 **Corollary 3.1.** *Let the matrices $G_{1,i}, \ldots, G_{n,i}$, $i = 1, \ldots, N$, be negative semi-definite. If*
86 $\mathrm{Re}(\lambda_\mathcal{A}) < 0$, *then the quadratic Markov jump system in (1) is second moment stable.*

87 **Remark 3.2.** *The novelty of Corollary 3.1 is that it reveals a easy-to-check condition*
88 *to verify the second moment stability of the quadratic system in (1), i.e., $\mathrm{Re}(\lambda_\mathcal{A}) < 0$,*
89 *a condition borrowed from [11, Thm 5.6], [7, Thm. 3.25, p. 52]. Thus, Corollary 3.1*
90 *expands the use of the matrix (6) for Markov jump systems with quadratic terms.*

91 **Remark 3.3.** *Corollary 3.1 has practical implications to design a real-time controller*
92 *subject to Markov jumps in an RLC circuit, where the corresponding experimental data*
93 *confirm the usefulness of Corollary 3.1, as detailed in Section 4.*
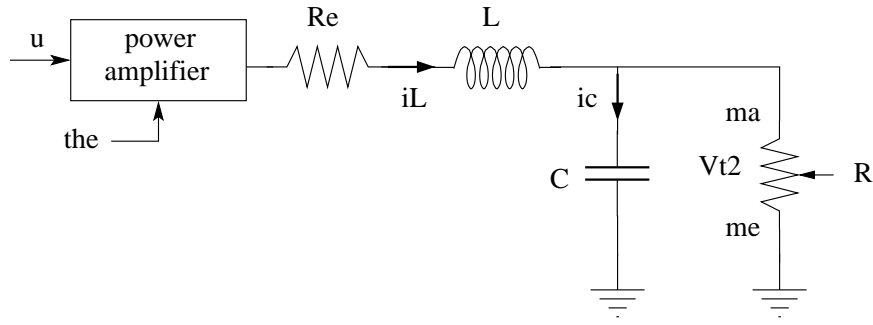
4

Figure 1: Open-loop diagram of the RLC circuit. The Markov chain generates jumps for both the power amplifier and the resistive load $R_{\theta(t)}$.

4. RLC circuit with Markov-driven load

Circuits based on resistor (R), inductor (L), and capacitor (C) are widely used in electrical equipments, such as antennas [2, 12], power converters [10, 13], filters [8], and oscilators [15]. In many of these applications based on RLC circuits, the load changes as the time evolves.

When electronic elements are connected or disconnected from the load terminals, the nominal value of the load changes accordingly. As such, time-varying loads induce time-varying voltages in the load terminals; but voltage fluctuations in terminals may represent risks of damage for the underlying devices. It is then necessary to keep the voltage supplied to the load at a fixed, regulated level.

The main contribution of this section is that of applying Corollary 3.1 to design a real-time controller for the RLC circuit. The aim of the controller is to regulate the voltage supplied to the load—the load value jumps according to a Markov chain. Actually, the proposed controller depends on quadratic terms. The benefits of such controller become clear through real-time experiments, as detailed next.

4.1. Modelling the RLC circuit with Markov jumps in the load

The RLC circuit studied in this section is detailed in Fig. 1. As can be seen, the RLC circuit has a power amplifier that converts the input signal $u(t)$ into the voltage-current required to supply the circuit. The output voltage, $v_o(t)$, is applied in the load $R_{\theta(t)}$; and the load $R_{\theta(t)}$ changes its value according to a Markov chain. In fact, three distinct resistive loads were used in the experiments, and the jumps among them were implemented through relays that were programmed to follow a three-state Markov chain.

To model the RLC circuit shown in Fig. 1, we consider a second-order system with two state variables (cf., [30]): (i) the current $i_L(t)$ flowing through the inductor; and (ii) the voltage $v_o(t)$ available in the terminals of the capacitor. It allows us to represent the RLC circuit through the next Markov jump system:

$$\mathrm{d} \begin{bmatrix} v_o(t) \\ i_L(t) \end{bmatrix} = \begin{bmatrix} -a_{11}^{(i)} & a_{12} \\ -a_{21} & -a_{22}^{(i)} \end{bmatrix} \begin{bmatrix} v_o(t) \\ i_L(t) \end{bmatrix} \mathrm{d}t + \begin{bmatrix} 0 \\ b^{(i)} \end{bmatrix} u(t)\mathrm{d}t + \begin{bmatrix} 0 \\ h \end{bmatrix} \mathrm{d}w(t), \qquad (7)$$
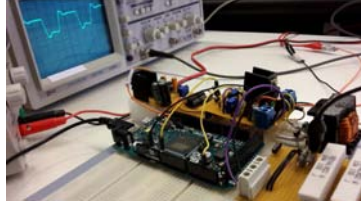
5

Figure 2: Laboratory testbed used to the experiments involving the RLC circuit.

116 with $\theta(t) = i \in \{1, 2, 3\}$, for each $t \geq 0$, where $a_{11}^{(i)}, a_{22}^{(i)}, b^{(i)}$, $i = 1, 2, 3$, and a_{12}, a_{21}, h are
117 positive numbers. These numbers were identified by the next procedure.

118 *4.2. Experiments for the identification of the RLC circuit*

119   A laboratory testbed was assembled to carry out the experiments involving the RLC
120 circuit, see Fig. 4.1. The laboratory was equipped with oscilloscopes, microcontrollers,
121 and power sources. A digital oscilloscope (Picoscope Model 2205) was used to measure
122 data from the input-output of the RLC circuit. In its input, the power amplifier received
123 analog signals from an Arduino Due. The Arduino Due was able to generate signals in $u(t)$
124 from 0V to 2.7V, and it worked with sampling time of 90 microseconds approximately.

125   In the experiments, the resistor $R_{\theta(t)}$ in the load assumed the value of $30\,\Omega$ when
126 $\theta(t) = 1$, $10\,\Omega$ when $\theta(t) = 2$, and $20\,\Omega$ when $\theta(t) = 3$. Relays were used to implement the
127 jumps among these resistances.

128   The power amplifier was assembled with an adjustable regulator, code LM338. A phe-
129 nomenon observed in the laboratory is that the internal resistance of the power amplifier
130 had changed its value slightly when the load changed. This phenomenon suggests that the
131 resistance of the power amplifier was also driven by the Markov jumps; this motivated us
132 to account the influence of such jumps in the element $b^{(i)}$ of the model (7).

133   In order to identify the parameters of (7), we calculated the mean square error between
134 the model in (7) and the corresponding experimental data (see Fig. 2). Square waves with
135 distinct amplitudes were applied in the input $u(t)$ of the RLC circuit in practice, and
136 the corresponding output data were compared with the values of $v_o(t)$ and $i_L(t)$ taken by
137 simulating (7); this comparison allowed us to find the parameters of (7) that minimized
138 that mean square error—these parameters are shown in Table 1.

139 *4.3. Markov jump control with quadratic terms*

140   Usually, RLC circuits must have a fixed voltage on the load under all operating condi-
141 tions, voltage condition referred to as *setpoint*. When a Markov jump occurs in the load,
142 the nominal value of the load changes, but changing the load creates a gap between the
143 desired setpoint and the voltage available in the load terminals—this voltage gap is called
144 *offset*.

145   Voltage offsets are undesired because they can lead not only to unnecessary loss of
146 energy, but also to damage of the underlying equipments. For instance, in transient
147 times, the equipment can suffer voltage spikes, exceeding safety limits. For this reason,
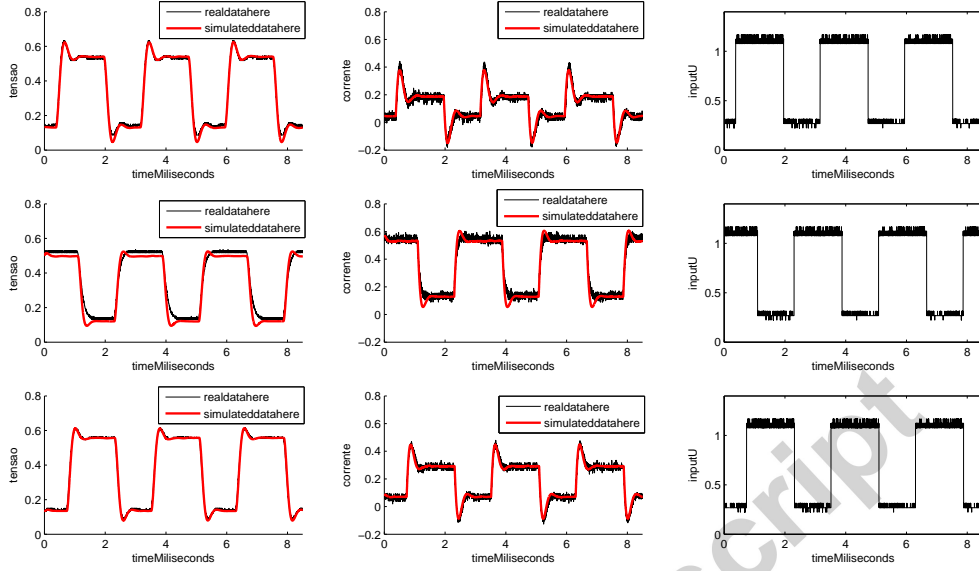
6

Figure 2: Data from the RLC circuit for a square wave input. Rows from up to down: $\theta(t) \equiv 1$, $\theta(t) \equiv 2$, and $\theta(t) \equiv 3$, respectively. The simulated curves were generated by using the values of Table 1.

it is reasonable to design controllers able to remove that voltage offsets, mainly for RLC circuits with jumping loads. Designing such a controller with the help of Corollary 3.1 sets the main contribution of this section.

The sensors used in the laboratory were designed to measure only the square of the output signals. This signifies that the sensors were used to measure $v_o(t)^2$ and $i_C(t)^2$. This feature lead us to construct a control signal $u(t)$ that depends on $v_o(t)^2$ and $i_C(t)^2$ only, as detailed next.

We mention that the load sensor presented a small bias of -50mV in practice, measured in the laboratory. For this reason, we set $\bar{v}_o(t) = v_o(t) + 0.05$ and adjusted the bias accordingly in $v_o(t)^2$.

Since the Proportional-Integrative (PI) control strategy has produced promising results in the control of processes subject to Markovian jumps [20, 17], we decided to adapt the PI control to our setup, as detailed in the scheme of Fig. 3. Note from Fig. 3 that the

Table 1: Parameters of the quadratic Markov jump system representing an RLC circuit.

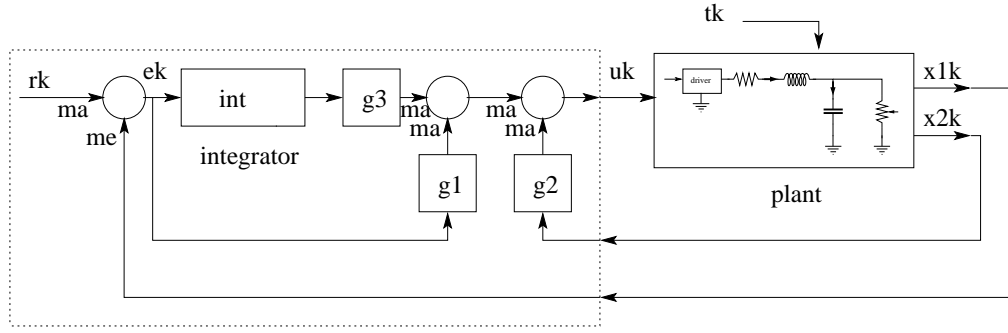| Parameters	$i = 1$	$i = 2$	$i = 3$
$a_{11}^{(i)}$	-3.98	-12.2492	-6.01
$a_{22}^{(i)}$	-7.167	-7.012	-8.3177
$b^{(i)}$	6.3415	8.101	7.4757
$a_{12} = 11.495$	$a_{21} = -10.651$	$h = 1$	

7

Figure 3: Block representing the 'proportional integrative' (PI) control strategy. The nonlinear feedback accounts both the square of voltage in the load and the square of current in the capacitor.

¹⁶¹ proposed control action is

$$u(t) = k_1 e(t) + k_2 \int_0^t e(\tau)\mathrm{d}\tau + k_3 i_C(t)^2, \quad e(t) = r(t) - \bar{v}_o(t)^2, \quad \forall t \geq 0, \qquad (8)$$

¹⁶² where $r(t)$ stands for a deterministic setpoint signal. With $r(t) \equiv r$, $r > 0$ being a constant
¹⁶³ to be given latter, the control objective was to assure that the statistical mean values of
¹⁶⁴ both $e(t)$ and $i_c(t)$ tend to zero as t tends to infinity.

Due to the Kirchhoff's current law, we can write $i_C(t) = i_L(t) - v_o(t)/R_{\theta(t)}$; hence

$$i_C(t)^2 = \begin{bmatrix} v_o(t) & i_L(t) \end{bmatrix} \begin{bmatrix} \frac{1}{R_{\theta(t)}^2} & \frac{-1}{R_{\theta(t)}} \\ \frac{-1}{R_{\theta(t)}} & 1 \end{bmatrix} \begin{bmatrix} v_o(t) \\ i_L(t) \end{bmatrix}. \qquad (9)$$

Now, take the system state as $x(t) \equiv [v_o(t)\ i_L(t)\ q(t)]'$; here $q(t)$ denotes the integral of the error, i.e., $q(t) := \int_0^t e(\tau)\mathrm{d}\tau$, so that $\dot{q}(t) \equiv e(t)$. Combining (7)–(9), we obtain the quadratic Markov jump system (with $\theta(t) = i$):

$$\mathrm{d}x(t) = \begin{bmatrix} -a_{11}^{(i)} & a_{12} & 0 \\ -a_{21} - 0.1b^{(i)}k_1 & -a_{22}^{(i)} & b^{(i)}k_2 \\ -0.1 & 0 & 0 \end{bmatrix} x(t)\mathrm{d}t + \begin{bmatrix} x(t)'G_{1,i}x(t) \\ x(t)'G_{2,i}x(t) \\ x(t)'G_{3,i}x(t) \end{bmatrix} \mathrm{d}t$$

$$+ \begin{bmatrix} 0 \\ b^{(i)}k_1(r(t) - 0.0025) \\ r(t) - 0.0025 \end{bmatrix} \mathrm{d}t + \begin{bmatrix} 0 \\ h \\ 0 \end{bmatrix} \mathrm{d}w(t), \quad (10)$$

where

$$G_{1,i} = 0, \quad G_{2,i} = b^{(i)} \begin{bmatrix} k_3/R_i^2 - k_1 & -k_3/R_i & 0 \\ -k_3/R_i & k_3 & 0 \\ 0 & 0 & 0 \end{bmatrix}, \quad G_{3,i} = \mathrm{diag}(-1, 0, 0), \quad i = 1, 2, 3.$$

¹⁶⁵ The controlled RLC circuit with Markov jumps in (10) satisfies the condition stated
¹⁶⁶ in Assumption 1.1. Indeed, for the RLC circuit assembled in our laboratory testbed, the
¹⁶⁷ output voltage $v_o(t)$ was greater than -1V as well as the current $i_L(t)$ was greater than

8

168 −1A for all $t \geq 0$. As a result, in (2), we considered $\mu_1 = -1$ and $\mu_2 = -1$ to cope (2)
169 with (10). To complete the analysis, we have assumed that $\mu_3 = -10$.

170 The Markov jumps on the load were programmed through relays, which followed the
171 next transition rate matrix:

$$\Pi = \begin{bmatrix} -53.0492 & 42.2072 & 10.8420 \\ 42.2072 & -53.0492 & 10.8420 \\ 54.2098 & 54.2098 & -108.4196 \end{bmatrix}.$$

172 Corollary 3.1 now plays a key role. In fact, with gains $(k_1, k_2, k_3) = (0.5, 0.05, -0.01)$ ar-
173 bitrarily chosen, we have that the corresponding matrix $\mathcal{A}$ in (6) yields $\mathrm{Re}(\lambda_{\mathcal{A}}) = -0.0097$.
174 Consequently, Corollary 3.1 assures that the quadratic Markov jump system in (10) is sec-
175 ond moment stable.

176 The remaining part of this section shows data collected from experiments that confirm
177 the second moment stability; this finding corroborates the usefulness of Corollary 3.1 for
178 the RLC circuit.

179 *4.4. Experimental results: controlled RLC circuit with Markov jumps*

180 The controlled RLC circuit with Markov jumps shown in Fig. 3 was assembled in the
181 laboratory testbed with control gains (k_1, k_2, k_3) as mentioned previously.

182 A small sample of data is shown in Fig. 4. The picture shows the output corresponding
183 to a step from 0V to 0.6V applied at $t = 1.5$ms, or equivalently, the reference was $r(t) = $
184 $r = 0.36\mathrm{V}^2$ when $t \geq 1.5$ms and zero otherwise. As can be seen in Fig. 4, the controller was
185 able to overcome the perturbations produced by the Markov jumps on the load, driving
186 the load voltage to the setpoint of 0.6V.

187 To assess the influence of the Markov jumps in the controlled RLC circuit, we analysed
188 the data taken from 12, 000 distinct experiments. Each experiment was carried out for a
189 step from 0V to 0.6V and execution time of 20ms. The experimental data were used to
190 generate the phase portrait depicted in Fig. 5.

191 Fig. 5 shows data for 12, 000 experiments. Since the jumps in the load produced
192 perturbations for both voltage and current, Fig. 5 represents the statistical dispersion of
193 these perturbations, accounted in the shading of the colors. As can be seen, the statistical
194 dispersion of voltage and current tends to follow an spiral path, in the clockwise direction,
195 and reach an accumulated point in 0.6V and 0A (colored in red in the middle of the
196 picture). This accumulated point represents the statistical mean.

197 In summary, Fig. 5 suggests that the controlled RLC circuit be second moment sta-
198 ble, an evidence that supports the result of Corollary 3.1—Corollary 3.1 states that the
199 quadratic system in (10) is second moment stable.

200 Our findings thus reinforce the usefulness of Corollary 3.1 for applications.

201 5. Concluding remarks

202 In this paper, we have presented conditions to assure the second moment stability of
203 Markov jump systems with quadratic terms. To prove our main result, we have borrowed
204 from [11, Thm 5.6], [7, Thm. 3.25, p. 52], a condition based on the spectral radius of
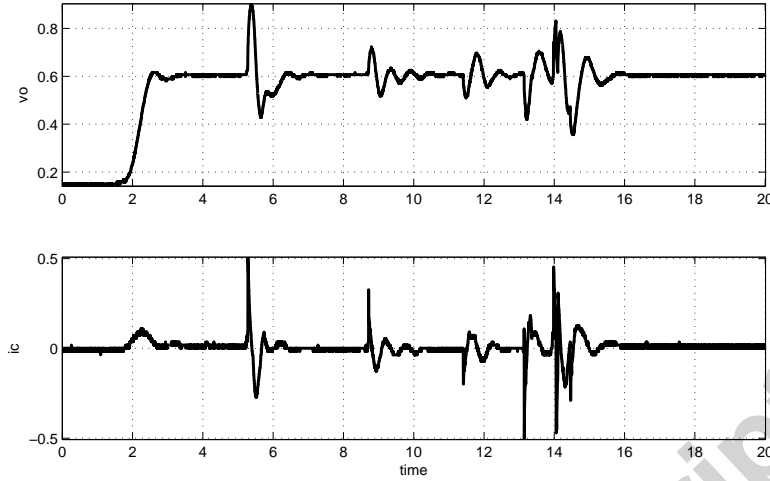
9

Figure 4: Typical response of the voltage in the load and current in the capacitor from a controlled RLC circuit subject to jumps on the load—the jumps driven by a Markov chain generated the perturbations. Even under perturbations, the proposed controller steered the load voltage to the desired setpoint (i.e., 0.6V).

the matrix in (6); and this condition is reinforced here to assure the stability of quadratic Markov jump systems (see both Assumption 1.1 and Corollary 3.1).

Besides the theoretical contributions, our findings have practical implications. Indeed, we have applied our stability result on the design of a real-time controller for an RLC circuit. The RLC circuit, assembled in a laboratory, supplied a resistive load with values jumping according to a Markov chain. Interestingly, the sensors used in practice to perform the control measured only the square of the corresponding variables (i.e., $v_o(t)^2$ and $i_C(t)^2$ in Fig. 3). This signifies that the control system resulted in a Markov jump system with quadratic terms.

Our main result, Corollary 3.1, was applied on the design of a second moment stabilizing controller for the RLC circuit—the experimental data suggested that the RLC circuit be second moment stable in practice. This evidence matches the theoretical result, a fact that supports the implications of our approach for applications.

Appendix: Proof of Theorem 3.1

In the next result, the notation $o(h)$ denotes an infinitesimal of higher order than h, i.e., $\lim_{h\downarrow 0} o(h)/h$ equals zero.

Proposition 5.1. *([11, Lem. 4.2], [7, Ch. 3]). Assume that $f(t)$ on $\mathbb{R}^{n\times m}$ is $\mathcal{F}_t$-measurable and that $f_i(t) := \mathrm{E}[f(t)\mathbb{1}_{\theta(t)=i}]$ exists. Then $\mathrm{E}[f(t)\mathrm{d}(\mathbb{1}_{\theta(t)=i})] = \sum_{j=1}^{N} \pi_{ji}f_j(t)\mathrm{d}t + o(\mathrm{d}t)$.*

Now, we are able to present the proof of Theorem 3.1.
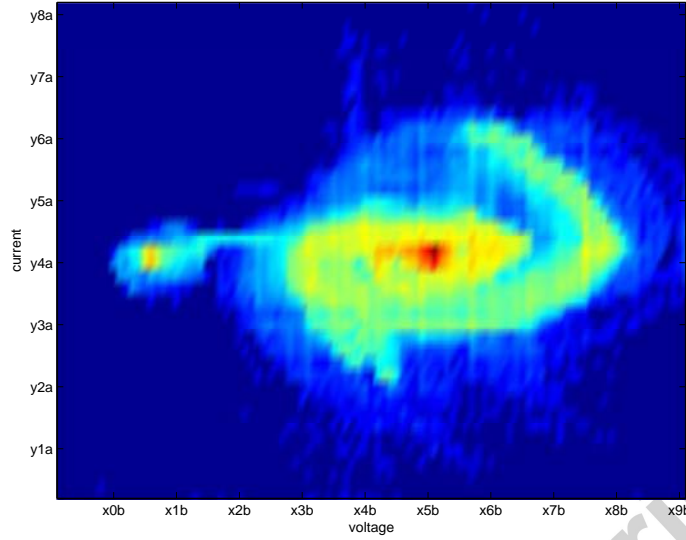
Proof. (Proof of Theorem 3.1).

10

Figure 5: Phase portraits representing the voltage in the load (V) and current in the capacitor (A) measured in practice from a RLC circuit with Markov jumps—the picture condenses data from $12,000$ distinct realizations. The picture suggests that the RLC circuit be second moment stable, a fact in accordance with Corollary 3.1.

₂₂₆ Before presenting the arguments to prove Theorem 3.1, we need first some definitions.
₂₂₇ Define the quadratic operator $\mathcal{G}_i : \mathbb{R}^n \mapsto \mathbb{R}^n$, $i = 1, \ldots, N$, as

$$\mathcal{G}_i(x) = \begin{bmatrix} x'G_{1,i}x \\ \vdots \\ x'G_{n,i}x \end{bmatrix}, \quad \forall x \in \mathbb{R}^n. \tag{11}$$

The next argument introduces the matrix differential equation for (3). Indeed, by applying the Itô's rule in (1), we can write $\mathrm{d}X_i(t)$ as (e.g., [7, Prop. 3.28, p. 56])

$$\mathrm{d}\,\mathrm{E}[x(t)x(t)'\mathbb{1}_{\theta(t)=i}] = \mathrm{E}[\mathrm{d}x(t)\,\mathrm{d}x(t)'\mathbb{1}_{\theta(t)=i}]$$
$$+ \mathrm{E}[\mathrm{d}x(t)\,x(t)'\mathbb{1}_{\theta(t)=i}] + \mathrm{E}[x(t)\,\mathrm{d}x(t)'\mathbb{1}_{\theta(t)=i}] + \mathrm{E}[x(t)x(t)'\,\mathrm{d}(\mathbb{1}_{\theta(t)=i})]. \tag{12}$$

₂₂₈ For the sake of clarity, each term in the right-hand side of (12) is evaluated in separate,
₂₂₉ as follows. The first term in the right-hand side of (12) reads as

$$\mathrm{E}[\mathrm{d}x(t)\,\mathrm{d}x(t)'\mathbb{1}_{\theta(t)=i}] = \mathrm{E}\left[H_{\theta(t)}\mathrm{d}w(t)\mathrm{d}w(t)'H'_{\theta(t)}\mathbb{1}_{\theta(t)=i}\right] = H_iH'_ip_i(t)\mathrm{d}t. \tag{13}$$

The second term in the right-hand side of (12) is identical to (using notation in (3))

$$\mathrm{E}[\mathrm{d}x(t)\,x(t)'\mathbb{1}_{\theta(t)=i}] = \mathrm{E}\left[\left(A_{\theta(t)}x(t) + \mathcal{G}_{\theta(t)}(x(t))\right)x(t)'\mathbb{1}_{\theta(t)=i}\right]\mathrm{d}t + \mathrm{E}[H_{\theta(t)}\mathrm{d}w(t)x(t)'\mathbb{1}_{\theta(t)=i}]$$
$$= A_iX_i(t)\mathrm{d}t + \mathrm{E}[\mathcal{G}_{\theta(t)}(x(t))x(t)'\mathbb{1}_{\theta(t)=i}]\mathrm{d}t. \tag{14}$$

₂₃₀ The last term in the right-hand side of (12) follows from Proposition 5.1, which assures
₂₃₁ that

$$\mathrm{E}[x(t)x(t)'\,\mathrm{d}(\mathbb{1}_{\theta(t)=i})] = \sum_{j=1}^{N} \pi_{ji}X_j(t)\mathrm{d}t + o(\mathrm{d}t). \tag{15}$$

11

Combining (12)–(15) yields

$$\dot{X}_i(t) = X_i(t)A_i' + A_i X_i(t) + \sum_{j=1}^{N} \pi_{ji} X_j(t) + H_i H_i' p_i(t)$$
$$+ \mathrm{E}\left[x(t)\mathcal{G}_{\theta(t)}(x(t))' \mathbb{1}_{\theta(t)=i}\right] + \mathrm{E}\left[\mathcal{G}_{\theta(t)}(x(t))x(t)' \mathbb{1}_{\theta(t)=i}\right]. \quad (16)$$

Note that the trace of the rightmost element of (16) equals

$$\mathrm{tr}\left\{\mathrm{E}\left[\begin{bmatrix} x(t)'G_{1,i}x(t) \\ \vdots \\ x(t)'G_{n,i}x(t) \end{bmatrix} \left[x_{[1]}(t),\ldots,x_{[n]}(t)\right] \mathbb{1}_{\theta(t)=i}\right]\right\}. \quad (17)$$

On the other hand, we have from (2) that given $\varepsilon > 0$, there exists some $t_0 \geq 0$ such that

$$\mu_\ell - \varepsilon < x_{[\ell]}(t), \quad \forall t \geq t_0, \ \ell = 1,\ldots, n.$$

Since the matrix $G_{\ell,i}$ is negative semi-definite by assumption, the value of $x_{[\ell]}(t)x(t)'G_{\ell,i}x(t)$ is bounded from above by $(\mu_\ell - \varepsilon)x(t)'G_{\ell,i}x(t)$ when $t \geq t_0$. Thus, we have from (17) that

$$\mathrm{tr}\left\{\mathrm{E}\left[\mathcal{G}_{\theta(t)}(x(t))x(t)' \mathbb{1}_{\theta(t)=i}\right]\right\} \leq \sum_{\ell=1}^{n} \mathrm{tr}\{\mathrm{E}[(\mu_\ell - \varepsilon)x(t)'G_{\ell,i}x(t)\mathbb{1}_{\theta(t)=i}]\}$$
$$= \sum_{\ell=1}^{n} \mathrm{tr}\{(\mu_\ell - \varepsilon)G_{\ell,i}X_i(t)\}. \quad (18)$$

Passing the trace operator on both sides of (16), and using (18), we obtain

$$\mathrm{tr}\left\{\dot{X}_i(t)\right\} \leq \mathrm{tr}\left\{X_i(t)\left(A_i + \sum_{\ell=1}^{n}(\mu_\ell - \varepsilon)G_{\ell,i}\right)' + \left(A_i + \sum_{\ell=1}^{n}(\mu_\ell - \varepsilon)G_{\ell,i}\right)X_i(t)\right.$$
$$\left. + \sum_{j=1}^{N} \pi_{ji} X_j(t) + H_i H_i' p_i(t)\right\}. \quad (19)$$

With $V(t)$ as in (4), $V(t_0) = X(t_0)$, we obtain $\mathrm{tr}\{X_i(t)\} \leq \mathrm{tr}\{V_i(t)\}$, for $i = 1,\ldots, N$, since $\varepsilon > 0$ was taken arbitrarily. The result then follows from (4) and (19). □

[1] Arnold, L., 1974. Stochastic differential equations: Theory and applications. Wiley-Interscience, Hoboken, NJ, USA.

[2] Best, S. R., Kaanta, B. C., 2009. A tutorial on the receiving and scattering properties of antennas. IEEE Antennas and Propagation Magazine 51 (5), 26–37.

[3] Boukas, E. K., 2006. Stochastic Switching Systems: Analysis and Design. Birkhäuser, Boston, USA.

[4] Brewer, J. W., 1978. Kronecker products and matrix calculus in system theory. IEEE Transactions on Circuits and Systems 25 (9), 772–781.

[5] Costa, E. F., Vargas, A. N., do Val, J. B. R., 2011. Quadratic costs and second moments of jump linear systems with general Markov chain. Math. Control Signals Systems 23 (1), 141–157.

[6] Costa, O. L. V., de Oliveira, A., 2012. Optimal mean-variance control for discrete-time linear systems with Markovian jumps and multiplicative noises. Automatica 48 (2), 304–315.

[7] Costa, O. L. V., Fragoso, M. D., Todorov, M. G., 2013. Continuous-Time Markov Jump Linear Systems. Series: Probability and Its Applications. Springer-Verlag, New York.

[8] Deliyannis, T., Sun, Y., Fidler, J. K., 1998. Continuous-Time Active Filter Design (Electronic Engineering Systems). CRC Press, Boca Raton, FL, USA.

[9] Dragan, V., Morozan, T., Stoica, A., 2004. H2 optimal control for linear stochastic systems. Automatica 40 (7), 31103–1113.

[10] Erickson, R. W., Maksimovic, D., 2001. Fundamentals of Power Electronics. Springer, New York, USA.

[11] Fragoso, M., Costa, O., 2005. A unified approach for stochastic and mean square stability of continuous-time linear systems with Markovian jumping parameters and additive disturbances. SIAM J. Control Optim. 44 (4), 1165–1191.

[12] Galehdar, A., Thiel, D. V., O'Keefe, S. G., 2007. Antenna efficiency calculations for electrically small, RFID antennas. IEEE Antennas and Wireless Propagation Letters 6, 156–159.

[13] Inam, W., Afridi, K. K., Perreault, D. J., 2014. High efficiency resonant DC/DC converter utilizing a resistance compression network. IEEE Trans. Power Electronics 29 (8), 4126–4135.

[14] Khasminskii, R. Z., Zhu, C., Yin, G., 2007. Stability of regime-switching diffusions. Stochastic Processes and their Applications 117 (8), 1037–1051.

[15] Lee, T. H., Hajimiri, A., 2000. Oscillator phase noise: a tutorial. IEEE Journal of Solid-State Circuits.

[16] Oliveira, R. C. L. F., Vargas, A. N., do Val, J. B. R., Peres, P. L. D., 2009. Robust stability, H2 analysis and stabilisation of discrete-time Markov jump linear systems with uncertain probability matrix. Internat. J. Control 82 (3), 470 – 481.

[17] Oliveira, R. C. L. F., Vargas, A. N., do Val, J. B. R., Peres, P. L. D., 2014. Mode-independent H2-control of a DC motor modeled as a Markov jump linear system. IEEE Trans. Control Systems Tech. 22 (5), 1915–1919.

[18] Shen, M., Yang, G.-H., 2012. H2 state feedback controller design for continuous Markov jump linear systems with partly known information. Int. J. Systems Science 43 (4), 786–796.

[19] Vargas, A. N., Bortolin, D. C., Costa, E. F., do Val, J. B. R., 2015. Gradient-based optimization techniques for the design of static controllers for Markov jump linear systems with unobservable modes. Int. J. Numer. Model. 28 (3), 239–253.

[20] Vargas, A. N., Costa, E. F., do Val, J. B. R., 2013. On the control of Markov jump linear systems with no mode observation: application to a DC motor device. Int. J. Robust Nonlinear Control 23 (10), 1136–115.

[21] Vargas, A. N., Furloni, W., do Val, J. B. R., 2013. Second moment constraints and the control problem of Markov jump linear systems. Numer. Linear Algebra Appl. 20 (2), 357–368.

[22] Xiong, J., Lam, J., Gao, H., Ho, D. W. C., 2005. On robust stabilization of Markovian jump systems with uncertain switching probabilities. Automatica 41 (5), 897 – 903.

[23] Yin, G., Xi, F., 2010. Stability of regime-switching jump diffusions. SIAM Journal on Control and Optimization 48 (7), 4525–4549.

[24] Yin, G. G., Zhu, C., 2010. Hybrid Switching Diffusions: Properties and Applications. Series: Stochastic Modelling and Applied Probability. Springer, New York, USA.

[25] Yin, Y., Shi, P., Liu, F., Lim, C. C., 2014. Robust control for nonhomogeneous markov jump processes: An application to {DC} motor device. Journal of the Franklin Institute 351 (6), 3322 – 3338.
    URL http://www.sciencedirect.com/science/article/pii/S0016003214000866

[26] Zhang, L., 2009. H_∞ estimation for discrete-time piecewise homogeneous Markov jump linear systems. Automatica 45 (11), 2570–2576.

[27] Zhang, L., Gao, H., Kaynak, O., 2013. Network-induced constraints in networked control systems – a survey. IEEE Trans. Industrial Informatics 9 (1), 403–416.

[28] Zhang, L., Lam, J., 2010. Necessary and sufficient conditions for analysis and synthesis of Markov jump linear systems with incomplete transition descriptions. IEEE Trans. Automatic Control 55 (7), 1695–1701.

[29] Zhang, L., Wang, C., Chen, L., 2009. Stability and stabilization of a class of multimode linear discrete-time systems with polytopic uncertainties. IEEE Transactions on Industrial Electronics 56 (9), 3684–3692.

[30] Zhao, X., Zhang, L., Shi, P., Karimi, H. R., 2014. Robust control of continuous-time systems with state-dependent uncertainties and its application to electronic circuits. IEEE Trans. Industrial Electronics 61 (8), 4161–4170.

[31] Zhao, Y., Gupta, V., 2015. Feedback stabilization of Bernoulli jump nonlinear systems: A passivity-based approach. IEEE Transactions on Automatic Control 60 (8), 2254–2259.

[32] Zhu, C., Yin, G., 2007. Asymptotic properties of hybrid diffusion systems. SIAM Journal on Control and Optimization 46 (4), 1155–1179.